Synthesis and Evaluation of the Estrogen Receptor β–Selective Radioligand 2-^{18}F-Fluoro-6-(6-Hydroxynaphthalen-2-yl) Pyridin-3-ol: Comparison with 16α-^{18}F-Fluoro-17β-Estradiol

Inês F. Antunes[1], Aren van Waarde[1], Rudi A.J.O Dierckx[1], Elisabeth G.E. de Vries[2], Geke A.P. Hospers[2], and Erik F.J. de Vries[1]

[1]Department of Nuclear Medicine and Molecular Imaging, University of Groningen, University Medical Center Groningen, Groningen, The Netherlands; and [2]Department of Medical Oncology, University of Groningen, University Medical Center Groningen, Groningen, The Netherlands

Estrogen receptors (ERs) are targets for endocrine treatment of estrogen-dependent cancers. The ER consists of 2 isoforms, ERα and ERβ, which have distinct biologic functions. Whereas activation of ERα stimulates cell proliferation and cell survival, ERβ promotes apoptosis. PET of ERα and ERβ levels could provide more insight in response to hormonal treatment. 16α-^{18}F-fluoro-17β-estradiol (^{18}F-FES) is a PET tracer for ER with relative selectivity for ERα. Here we report the synthesis and evaluation of a potential ERβ-selective PET tracer: 2-^{18}F-fluoro-6-(6-hydroxynaphthalen-2-yl)pyridin-3-ol (^{18}F-FHNP). **Methods:** ^{18}F-FHNP was synthesized by fluorination of the corresponding nitro precursor, followed by acidic removal of the 2-methoxyethoxymethyl protecting group. In vitro affinity of ^{18}F-FHNP and ^{18}F-FES for ER was evaluated in SKOV3 ovarian carcinoma cells. PET imaging and ex vivo biodistribution studies with ^{18}F-FHNP and ^{18}F-FES were conducted in athymic nude mice bearing a SKOV3 xenografts. **Results:** ^{18}F-FHNP had nanomolar affinity for ERs, with a 3.5 times higher affinity for ERβ. ^{18}F-FHNP was obtained in 15%–40% radiochemical yield (decay-corrected), with a specific activity of 279 ± 75 GBq/μmol. ^{18}F-FHNP had a dissociation constant of 2 nM and maximum binding capacity of 18 fmol/10^6 cells, and ^{18}F-FES had a dissociation constant of 3 nM and maximum binding capacity 83 fmol/10^6 SKOV3 cells. Both ^{18}F-FHNP and ^{18}F-FES PET could clearly visualize the tumor in male mice bearing a SKOV3 xenograft. Biodistribution studies showed similar distribution of ^{18}F-FHNP and ^{18}F-FES in most peripheral organs. ^{18}F-FES showed a 2-fold-higher tumor uptake than ^{18}F-FHNP. The tumor-to-plasma ratio of ^{18}F-FES decreased 55% (P = 0.024) and 8% (P = 0.68) when administered in the presence of estradiol (nonselective) and genistein (ERβ-selective), respectively. The tumor-to-plasma ratio of ^{18}F-FHNP decreased 41% (P = 0.004) and 64% (P = 0.0009) when administered with estradiol and genistein, respectively. **Conclusion:** The new PET tracer ^{18}F-FHNP has suitable properties for imaging and shows relative selectivity for ERβ.

Key Words: estrogen receptors; hormones; PET; imaging; cancer

J Nucl Med 2017; 58:554–559
DOI: 10.2967/jnumed.116.180158

Estrogens play a central role not only in the growth, development, and maintenance of a diverse range of healthy tissues, but also in hormone-regulated cancers, including breast, ovarian, and prostate (*1*). The effects of estrogens are mediated through 2 receptors, estrogen receptor α (ERα) and β (ERβ), which operate as ligand-dependent transcription factors that modulate oncogenesis and tumor suppressor gene activation. Inhibition of hormone receptor signaling can be an effective treatment in hormone-regulated cancer (*2*), provided that these receptors are actually expressed by the tumors.

ERα and ERβ have distinct biologic functions and their levels can vary in both normal tissue and tumors. Although ERβ is expressed in breast, ovarian, and prostate tissues, ERα is usually the major subtype in cancers derived from these organs, with ERβ levels decreasing as the cancer progresses (*3*). In general, activation of ERα by estrogens stimulates cell proliferation and cell survival in tumors. Signaling via the ERβ is thought to be antiproliferative and to promote apoptosis in cancer since ERβ can inhibit ERα signaling by forming ERα–ERβ heterodimers (*4*). Because of the opposite effects induced by ERα and ERβ, a tool to determine the ER phenotype of all tumors in the body would be of great interest. Currently, ER expression and phenotype are usually determined ex vivo in a biopsy of the primary tumor. However, ER status of metastases may differ from the primary tumor. In addition, receptor expression by the tumor can change over time, either spontaneously or due to treatment. Crosstalk of the ER with the growth factor receptors is an important factor leading to the treatment-induced changes in ER expression (*5,6*).

PET can noninvasively generate whole-body images of receptor expression and thus can be used to monitor the ER status of all tumor lesions in a patient. The images could guide clinicians in therapeutic decision making. Currently, 16β-^{18}F-fluoro-16α-estradiol (^{18}F-FES) is used as a PET tracer for the clinical assessment of the ER status in patients with a clinical dilemma (*7,8*). In a high percentage of the patients, ^{18}F-FES PET actually caused a change in treatment regimen, indicating that ER imaging can indeed have

Received Jul. 7, 2016; revision accepted Nov. 26, 2016.
For correspondence or reprints contact: Inês F. Antunes, Department of Nuclear Medicine and Molecular Imaging, University Medical Center Groningen, University of Groningen, P.O. Box 30.001, 9700 RB Groningen, The Netherlands.
E-mail: i.farinha.antunes@umcg.nl
Published online Dec. 1, 2016.

an important impact on patient management (*8*). However, ^{18}F-FES possesses a weak subtype selectivity (ERα/ERβ = 2.5) (*9*). Therefore, ^{18}F-FES PET can provide accurate information about ER expression, but not about the ER phenotype. Subtype-selective tracers would allow the assessment of the ERβ/ERα ratio, offering a better characterization of tumor lesions and therefore a better assessment of the stage of the disease and its sensitivity toward different endocrine therapies. Most important, the ERβ subtype tracers could be used in the assessment of the ERβ in lung carcinomas (*10*) and lung fibrosis (*11*) where ERβ is known to be involved in these diseases. Unfortunately, PET tracers with high subtype selectivity for ERβ or ERα are currently unavailable.

Recently, Mewshaw et al. reported a series of phenylnaphthalene compounds with good ERβ/ERα selectivity (*12*). On the basis of the properties of this series of phenylnaphthalene analogs, we selected 6-(3-fluoro-4-hydroxyphenyl)naphthalene-2-ol, with an ERβ/ERα selectivity of 17, as a lead compound for development of a PET tracer for ERβ imaging.

Radiolabeling of this compound for PET imaging could theoretically be achieved by a nucleophilic aromatic substitution reaction of the corresponding aromatic nitro or quaternary ammonium compound with ^{18}F-fluoride. However, this reaction only proceeds well if the electron density of the benzene ring is sufficiently reduced by a strong electron-withdrawing group. Unfortunately, our lead compound does not contain electron-withdrawing substituents and therefore cannot be labeled in this manner. Nowadays, several new approaches are in development that would allow direct fluorination of electron-rich aromatic rings, using, for example, iodonium salts, sulfonium salts, and boronic acids (*13,14*). On the other hand, nucleophilic aromatic fluorination reactions of 2-nitropyridines with ^{18}F-fluoride are facile and give high labeling yields (*15*). We selected this strategy as first approach to develop a PET tracer for ERβ. Therefore, the pyridine analog of our lead compound, FHNP, was selected as a candidate PET tracer for ERβ imaging. Herein, we describe the synthesis and biologic evaluation of ^{18}F-FHNP (2-^{18}F-fluoro-6-[6-hydroxynaphthalen-2-yl]pyridin-3-ol) (Fig. 1).

MATERIALS AND METHODS

The synthesis and characterization of unlabeled FHNP and the nitro precursor (Supplemental Figures 1 and 2 [available at http://jnm.snmjournals.org]) are presented in the supplemental materials.

^{18}F-FES was produced as previously described (*16*). The lipophilicity $LogD_{7.4}$ studies were performed as previously described (*17*).

The in vitro binding affinity of FHNP toward ERα and ERβ (*18*) was determined by a competitive radiometric binding assay using ^{3}H-estradiol as the ligand (Supplemental Table 1).

PET image reconstruction, data analysis, and ex vivo biodistribution were performed as previously described (*19*). Tracer uptake was expressed as percentage injected dose per gram (%ID/g).

The Western blotting was performed according to the literature (*20*).

Radiosynthesis of ^{18}F-FHNP

Aqueous ^{18}F-fluoride was produced by irradiation of ^{18}O-water with a Scanditronix MC-17 cyclotron via the ^{18}O(p,n)^{18}F nuclear reaction. The ^{18}F-fluoride solution was passed through a QMA SepPak Light anion exchange cartridge (Waters) to recover the ^{18}O-water. The ^{18}F-fluoride was eluted from the cartridge with 1 mL of K_2CO_3 (5 mg/mL) and collected in a vial with 15 mg of kryptofix[2.2.2]. To this solution, 1 mL of acetonitrile was added, and the solvents were evaporated at 130°C. The ^{18}F-KF/kryptofix complex was dried 3 times by the addition of 0.5 mL of acetonitrile, followed by evaporation of the solvent. A solution of 3-((2-methoxyethoxy)methoxy)-6-(6-((2-methoxyethoxy)methoxy)naphthalene-2-yl)-2-nitropyridine (1 mg, 2.1 mmol) in 0.5 mL of dry dymethylsulfoxide was added to the ^{18}F-KF/kryptofix complex. The reaction mixture was heated at 150°C for 15 min. After the mixture was allowed to cool down to 90°C, 1 mL of 2 M HCl was added and the reaction mixture was heated at 90°C for 15 min to remove the 2-methoxyethoxymethyl groups. The product was purified by high-performance liquid chromatography (column: Luna C18;5 μm, 250 × 4.6 mm; eluent: 30% acetonitrile in 0.025 M phosphate-buffered saline, pH 7; flow: 4 mL/min; retention time, ^{18}F-FHNP = 24 min). The radioactive peak corresponding to the product was collected and diluted with 50 mL of distilled water and passed through a C18 SepPak light cartridge (Waters, conditioned with 5 mL of ethanol and 10 mL of water). The product was eluted from the cartridge with 0.7 mL of ethanol, followed by 5 mL of distilled water. Quality control was performed by ultra-performance liquid chromatography, using a HSS T3 column (1.8 μm, 3.0 × 50 mm) with 30% aqueous acetonitrile as the mobile phase at a flow of 1 mL/min (retention time, ^{18}F-fluoride = 0.5 min, ^{18}F-FHNP = 2.1 min).

Stability of ^{18}F-FHNP

Samples of ^{18}F-FHNP dissolved in formulated eluent (1 mL) were analyzed after 60 min at room temperature by ultra-performance liquid chromatography.

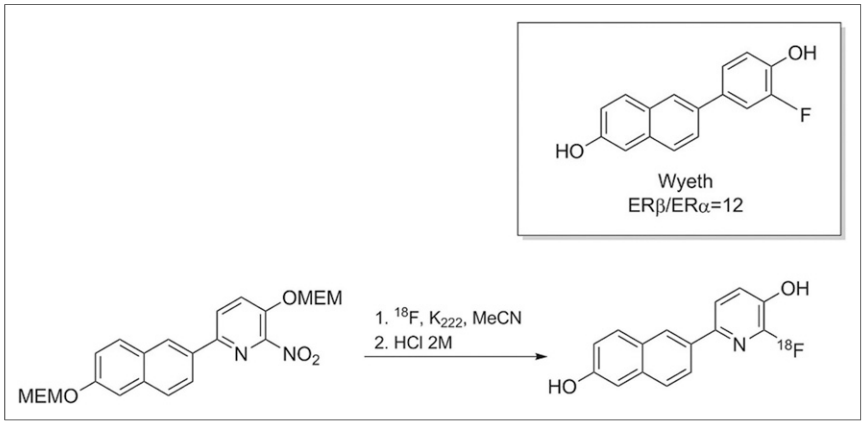

FIGURE 1. (Top) Structure of ERβ phenylnaphthalene-core ligand. (Bottom) Radiosynthesis of ^{18}F-FHNP.

Animals

Athymic male nude mice (age, 6–8 wk, n = 36; Harlan Laboratories) were used to avoid high variability of endogenous estradiol levels. All studies were performed in compliance with the Dutch regulations for animal experiments. The protocol was approved by the Institutional Animal Care and Use Committee (protocol no. DEC 6657A). After 1 wk of acclimatization, SKOV3 cells (1 to 2 × 10^6 cells in a 1:1 mixture of Matrigel and Dulbecco modified Eagle medium-high with 10% fetal bovine serum) were subcutaneously injected into the upper back of the mice. When palpable tumor nodules were formed, the animals were divided in 2 groups: injected with ^{18}F-FES and injected with ^{18}F-FHNP.

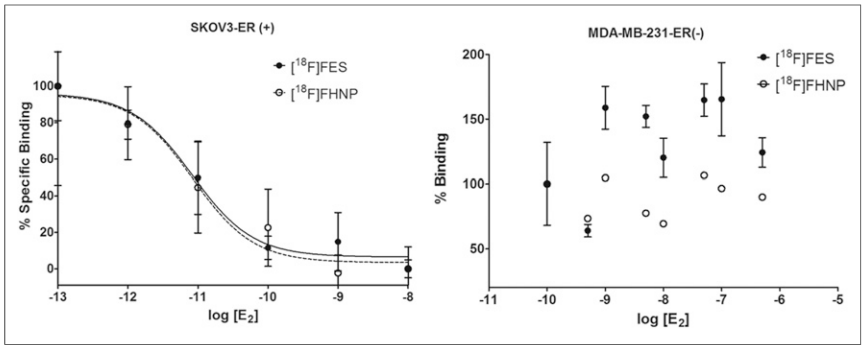

FIGURE 2. In vitro competitive ER binding assay of ^{18}F-FHNP and ^{18}F-FES in SKOV3 and MDA-MB-231 cells, using estradiol (E2) as competitor. Data are presented as mean ± SEM of samples obtained in triplicate. Specific binding was obtained by subtracting nonspecific binding (residual binding of tracer in presence of highest dose of competing drug) from total binding, representing 60%–80% of total uptake by SKOV3 cells.

Pet Imaging in Mice Bearing Skov3 Xenograft

On day 15 after SKOV3 cell inoculation, the mice were anesthetized with 2% isoflurane and positioned in the center of the field of view of the small-animal PET camera (Focus 220; Siemens-Concorde) in a transaxial position. ^{18}F-FES (14 ± 7 MBq) or ^{18}F-FHNP (9 ± 4 MBq) was mixed with either phosphate-buffered saline (control) or estradiol (nonselective ER ligand, 0.3 μg/g animal) and injected via the penile vein of the animal. In a subset of control animals, genistein (ERβ-selective ligand, 5 μg/g animal) was intraperitoneally administered 5 min before tracer injection. Simultaneously with the injection of the PET tracer, a 60-min dynamic emission scan was started. After the PET scan was completed, a 15-min transmission scan with a ^{57}Co point source was obtained for the correction of scatter and attenuation of 511 keV photons by tissue. Once the transmission scan was concluded, the animals were terminated with an overdose of anesthesia. The animals remained fixed to the bed during the transmission scan, and then were transferred onto the bed of the CT scanner (Micro-CT II; CTI Siemens). A 15-min CT scan was acquired for anatomic localization of the tumor (*19*).

Immunohistochemistry

Formalin-fixed, paraffin-embedded SKOV3 tumor sections were deparaffinized in xylene, rehydrated, and incubated overnight with the rabbit monoclonal anti-ERα (ab32063) or mouse monoclonal anti-ERβ (ab16813) primary antibody. The next day the slides were incubated with a secondary biotinylated antibody, 3,3′-diaminobenzidine tetrahydrochloride for the visualization of the antibody–enzyme complex. The counterstaining was performed with hematoxylin/blue reagent. Positive cells presented a brownish color whereas negative controls and unstained cells became blue.

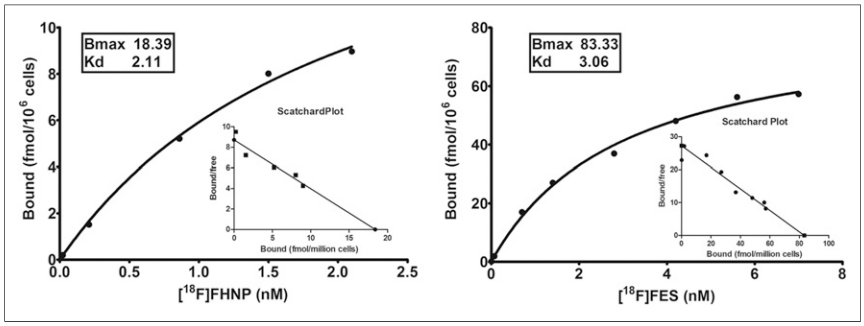

FIGURE 3. Scatchard plots for ^{18}F-FHNP and ^{18}F-FES binding in SKOV3 cells (n = 1, triplicate).

Statistical Analysis

The dissociation constant (K_D), maximum binding capacity (B_{max}), and 50% inhibition of tracer binding (IC_{50}) values were determined with GraphPad Prism (version 5.04; GraphPad Software). Differences in tracer accumulation between groups were analyzed using the 2-sided unpaired Student t test. Significance was reached when the P value was less than 0.05. Data are presented as mean ± SD unless stated otherwise.

RESULTS

Radiochemistry

^{18}F-FHNP was obtained in a 15%–40% radiochemical yield (decay-corrected) within 130 min. At the end of synthesis, the specific activity was 279 ± 75 GBq/μmol, and the radiochemical purity was always higher than 95%. ^{18}F-FES was obtained in a 15% ± 8% decay-corrected radiochemical yield. The specific activity of ^{18}F-FES was 244 ± 112 GBq/μmol, with a radiochemical purity of 99.9% ± 0.2%. ^{18}F-FHNP and ^{18}F-FES were stable for at least 60 min, because no decomposition was observed by ultra-performance liquid chromatography analysis. The distribution coefficients (logD, octanol/phosphate buffer pH 7.4) of ^{18}F-FHNP and ^{18}F-FES were 1.85 ± 0.01 and 2.50 ± 0.01, respectively.

In Vitro Binding Affinity

The in vitro binding affinity of ^{18}F-FHNP and ^{18}F-FES toward ER was evaluated in ER-negative MDA-MB-231 and ER-positive SKOV3 cells (Fig. 2), using different concentrations of the competitive inhibitor estradiol. The estradiol concentration that inhibited 50% of tracer binding (IC_{50}) was 8.5 and 8.3 pM for ^{18}F-FHNP and ^{18}F-FES in SKOV3 cells, respectively.

When SKOV3 cells were incubated with increasing amounts of ^{18}F-FHNP and ^{18}F-FES, saturation curves were obtained. The Scatchard plot obtained from these saturation curves (Fig. 3) provided a K_D of 2 nM and B_{max} of 18 fmol/10^6 cells for ^{18}F-FHNP and a K_D of 3 nM and B_{max} of 83 fmol/10^6 cells for ^{18}F-FES.

The in vitro selectivity of ^{18}F-FHNP toward ERα and ERβ was determined by a competitive radiometric binding assay using ^{3}H-estradiol as the ligand (*18*). The binding affinities of ^{18}F-FHNP for ERα and ERβ were 1.5% and 5.2%, respectively, relative to estradiol. Thus, ^{18}F-FHNP showed an approximately 3.5-times-higher selectivity for ERβ than for ERα in this assay (Supplemental Table 1).

^{18}F-FES binding assays in SKOV3 cells with different concentrations of subtype-selective ligands gave comparable IC_{50} values for the ERα antagonist fulvestrant (6.8 pM) (*21*) and the ERβ agonist genistein (8.5 pM) (*22*). When ^{18}F-FHNP was used as the radioligand, a 5-fold-higher IC_{50} value (38 pM) was obtained for fulvestrant, whereas a 10-fold-lower IC_{50} value (0.8 pM) was observed for genistein (Supplemental Fig. 3).

In Vivo PET Imaging

^{18}F-FHNP and ^{18}F-FES PET scans were obtained in SKOV3 tumor–bearing athymic nude mice injected with vehicle or the ER ligands estradiol or genistein (Fig. 4).

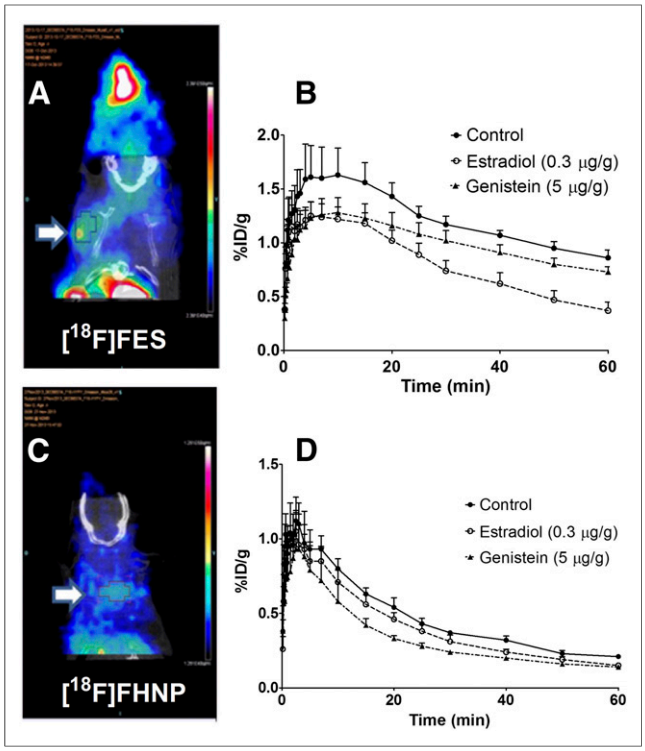

FIGURE 4. Coronal small-animal PET/CT fusion images of 2 mice bearing a SKOV3 xenograft (white arrows) injected with ^{18}F-FES (14 ± 7 MBq) (A) or ^{18}F-FHNP (9 ± 4 MBq) (C). Time–activity curves of tumor uptake (%ID/g) of ^{18}F-FES (B) and ^{18}F-FHNP (D) in SKOV3 xenografts.

The time–activity curves of the tumors revealed faster kinetics for ^{18}F-FHNP than for ^{18}F-FES. The accumulation of ^{18}F-FHNP in the tumors of control mice reached a maximum 2.5 min after injection and subsequently decreased exponentially with a half-life of 20 ± 4 min. In contrast, the accumulation of ^{18}F-FES in the tumors of control mice reached a maximum 10 min after injection and afterward decreased exponentially, with a half-life of 60 ± 30 min. The tracer accumulation in tumors obtained from the last 10 min of the PET scan (50–60 min) were 0.86 ± 0.18 %ID/g for ^{18}F-FES and 0.21 ± 0.03 %ID/g for ^{18}F-FHNP. Injection of ^{18}F-FES together with estradiol resulted in a significant reduction in tumor uptake (0.38 ± 0.18 %ID/g, $P < 0.05$), whereas genistein did not significantly affect ^{18}F-FES uptake (0.73 ± 0.12 %ID/g, $P = 0.33$). Likewise, estradiol—but not genistein—significantly reduced the area under the time–activity curve of the tumor ($P = 0.048$) (Supplemental Fig. 4). Tumor uptake of ^{18}F-FHNP, on the other hand, was significantly decreased by both estradiol (0.12 ± 0.07 %ID/g, $P < 0.05$) and genistein (0.15 ± 0.01 %ID/g, $P < 0.05$). The area under the curve, however, was only significantly reduced by genistein ($P = 0.033$).

Ex Vivo Biodistribution

In SKOV3 xenograft–bearing mice, ^{18}F-FHNP exhibited a biodistribution similar to ^{18}F-FES in most peripheral organs, with the highest uptake in the liver, kidneys, and urine at 1 h after injection (Figs. 5 and 6). ^{18}F-FES showed an approximately 2-times-higher tumor uptake (1.32 ± 0.66 %ID/g) than ^{18}F-FHNP (0.57 ± 0.07 %ID/g) (Supplemental Tables 2 and 3). ^{18}F-FHNP uptake in the excised tumors was significantly lower in animals that were injected with estradiol (0.45 ± 0.10 %ID/g, $P < 0.05$) or genistein (0.30 ± 0.08 %ID/g, $P < 0.001$). In contrast, ^{18}F-FES uptake in the excised tumors was only significantly reduced in animals that were coinjected with estradiol (0.56 ± 0.35 %ID/g, $P < 0.05$), but not in mice that were injected with genistein (1.11 ± 0.39 %ID/g, $P = 0.52$). Likewise, the tumor-to-plasma ratio of ^{18}F-FHNP (0.55 ± 0.12) was significantly reduced after injection with estradiol (0.33 ± 0.06, $P < 0.01$) or genistein (0.20 ± 0.06, $P < 0.001$), whereas the tumor-to-plasma ratio of ^{18}F-FES (1.16 ± 0.48) was only significantly reduced when coinjected with estradiol (0.53 ± 0.22, $P < 0.05$).

Immunohistochemistry

To confirm the expression of both ER subtypes in SKOV3 xenografts, tumors were sectioned and stained for ERα and ERβ expression. As shown in Figure 7, the SKOV3 tumors expressed both ERα and ERβ, although ERα is more abundant than ERβ.

Western Blotting

Western blotting was performed to evaluate the ERα and ERβ expression in the SKOV3 xenografts. Immunoreactive bands for ERα and ERβ were visualized at 65 and 55 KDa, respectively (Supplemental Fig. 5). As shown in Figure 7D, SKOV3 tumors expressed significantly higher amounts of ERα than ERβ ($P = 0.048$).

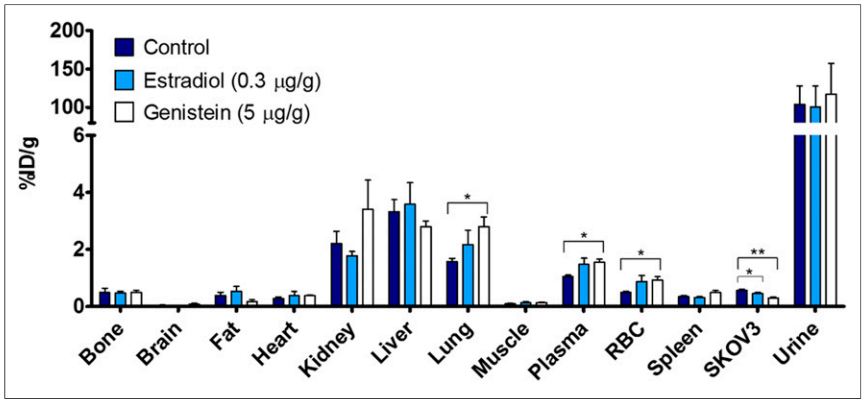

FIGURE 5. Biodistribution 1 h after intravenous injection of ^{18}F-FHNP in mice bearing a SKOV3 tumor xenograft. Competition studies were performed by injection of tracer with either estradiol (intravenously) or genistein (intraperitoneally). Data are expressed as %ID/g (mean ± SEM). Statistically significant differences between treated and control animals, $^{*}P < 0.05$ and $^{**}P < 0.001$.

DISCUSSION

Selective PET imaging of ERβ or ERα expression in endocrine tumors may provide a useful molecular assessment of the stage of the disease and its sensitivity toward various endocrine therapies and therefore might help in the selection of the most appropriate therapies for each individual patient. In this study, we developed the ^{18}F radioligand ^{18}F-FHNP for imaging ERβ and compared it with the standard PET tracer ^{18}F-FES, which is known for its preferential affinity toward ERα.

The optimized radiolabeling of ^{18}F-FHNP consisted of a 1-pot 2-step fluorination–deprotection procedure, leading to the desired product with a specific activity similar

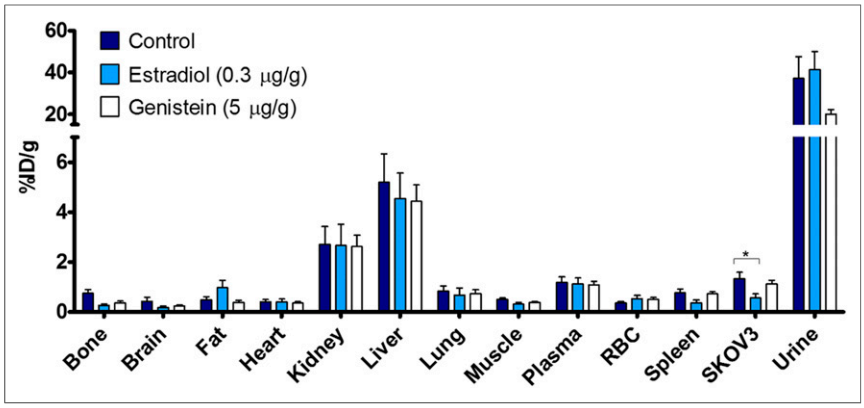

FIGURE 6. Biodistribution 1 h after intravenous injection of ^{18}F-FES in mice bearing SKOV3 tumor xenograft. Competition studies were performed by injection of tracer with either estradiol (intravenously) or genistein (intraperitoneally). Data are expressed as %ID/g (mean ± SEM). Statistically significant differences between treated and control animals, $^*P < 0.05$.

to ^{18}F-FES. Although ^{18}F-FHNP does not possess a steroidal structure, it was found that it had a lipophilicity (1.85 ± 0.01) similar to ^{18}F-FES (2.50 ± 0.01).

Besides being stable and having adequate lipophilicity and high specific activity, a suitable PET tracer must also have a high affinity toward ER, and in this case a high selectivity toward ERβ. Thus, to evaluate ^{18}F-FHNP affinity toward ER and compare it with ^{18}F-FES, a competitive radiometric binding assay was performed with both tracers in SKOV3 (ER-positive) and MDA-MB-231 (ER-negative) cells. As expected, ^{18}F-FHNP and ^{18}F-FES binding were displaced by estradiol only in SKOV3 cells, demonstrating that ^{18}F-FHNP and ^{18}F-FES have affinity toward the total ER population. This was further confirmed with a Scatchard plot, providing similar dissociation constants in a nanomolar range for both tracers. However, B_{max} obtained for ^{18}F-FHNP in SKOV3 cells was 5-fold lower than for ^{18}F-FES. This low B_{max} value obtained for ^{18}F-FHNP may be explained by the low levels of ERβ, which were confirmed by immunohistochemistry and Western blotting.

To confirm ERβ selectivity, a binding assay was performed with ERα and ERβ using ^{3}H-estradiol as the ligand, showing a 3.5-times-higher selectivity of FHNP for ERβ. This value is lower than the reported value for 6-(3-fluoro-4-hydroxyphenyl)-naphthalene-2-ol (ERβ/ERα = 17), indicating that the substitutions of the phenyl ring with a pyridine ring may have decreased the selectivity of ^{18}F-FHNP for ERβ.

In an attempt to further prove the ERβ selectivity of ^{18}F-FHNP, different subtype-selective ligands were used in a competitive binding assay. As depicted in Supplemental Figure 3, genistein competes stronger (lower IC_{50}) with ^{18}F-FHNP than with ^{18}F-FES, whereas fulvestrant competes stronger with ^{18}F-FES than with ^{18}F-FHNP. This is in agreement with ^{18}F-FES being more selective for the same subtype as fulvestrant (ERα) and ^{18}F-FHNP being more selective for the same subtype as genistein (ERβ).

To evaluate the potential of ^{18}F-FHNP as a PET tracer for in vivo imaging of ERβ expression, dynamic PET scans were obtained in the SKOV3 tumor–bearing athymic nude mice. The SKOV3 tumors can grow independent of endogenous or exogenous estradiol, because SKOV3 xenografts are known to express human epidermal growth factor receptor-2 in addition to ERα/ERβ, and therefore tumor growth can be stimulated via the express human epidermal growth factor receptor-2 pathway. In fact, we were able to grow SKOV3 xenografts in male athymic nude mice without the use of estrogen pellets. A major advantage of this model is that the levels of circulating estradiol are low and therefore competition of endogenous estradiol with the tracer for the ER binding site is negligible.

The ex vivo biodistribution studies at 1 h after tracer injection showed similar distributions of ^{18}F-FHNP and ^{18}F-FES in most peripheral organs. Uptake in bone was low, indicating minimal defluorination for both tracers. The highest tracer accumulation for both tracers was in the excretion organs. The accumulation of ^{18}F-FHNP in urine was 3 times higher than ^{18}F-FES, whereas similar radioactivity levels were found in other excretion organs (liver and kidneys) for both tracers. The higher accumulation of ^{18}F-FHNP in the urine can be attributed to the lower lipophilicity of ^{18}F-FHNP, resulting in less nonspecific binding and faster renal clearance. This could also explain the 2-times-lower tumor accumulation of ^{18}F-FHNP than ^{18}F-FES. Results obtained from PET imaging (Fig. 4) were similar to those obtained from ex vivo biodistribution.

The time–activity curves of control mice revealed that tumor washout of ^{18}F-FHNP was faster than the tumor clearance of ^{18}F-FES. However, one cannot ascribe the faster tumor washout of ^{18}F-FHNP with certainty to a lower in vivo affinity of the tracer for the ERs than ^{18}F-FES, because tumor uptake is also determined by other factors, such as receptor expression levels, tracer delivery, and nonspecific binding. In fact, immunohistochemistry and Western blotting (Fig. 7) revealed that the SKOV3 xenografts have a lower expression of ERβ than ERα, which is in agreement with the literature (*23*). With less binding sites available for a ERβ-selective tracer, the retention of ^{18}F-FHNP is indeed expected to be less than the retention of the ERα-selective tracer ^{18}F-FES.

To investigate the specificity of tracer uptake in ER-positive tumors in vivo, binding sites were saturated by administration of the nonselective ER ligand estradiol or the ERβ-selective

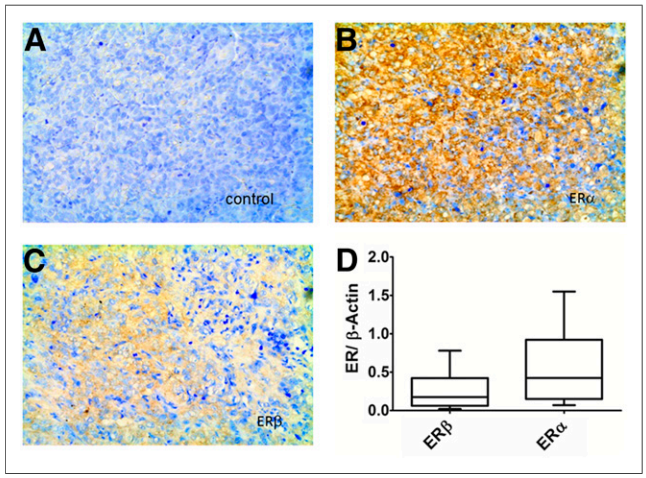

FIGURE 7. Representative immunostaining of SKOV3 xenografts (20× amplification) for control (n = 1,10 slices) (A), ERα (n = 2, 15 slices) (B), and ERβ (n = 2, 15 slices) (C). (D) Average ER protein–to-β–actin ratio values of single Western blotting experiment ($^*P < 0.05$).

compound genistein. Injection of ^{18}F-FES with estradiol resulted in a significant reduction in tumor uptake, whereas genistein did not significantly affect ^{18}F-FES uptake. Because genistein is an ERβ-selective ligand, it binds less to ERα and as a result it cannot compete with ^{18}F-FES binding to ERα. Given the low ERβ expression levels in SKOV3 xenografts, the reduction in ^{18}F-FES uptake after administration of genistein is expected to be less pronounced than the reduction in the tumor uptake when the tracer is coinjected with estradiol. Tumor uptake of ^{18}F-FHNP, on the other hand, was significantly decreased by both estradiol and genistein, suggesting that ^{18}F-FHNP is predominantly bound to ERβ in SKOV3 xenografts in vivo.

Interestingly, animals that were injected with ER blockers had significantly higher plasma levels of ^{18}F-FHNP, which eventually leads to higher tracer delivery of the tracer to the tumor. Nevertheless, a significant reduction of ^{18}F-FHNP uptake in tumors was found after injection of an ER blocker, which clearly shows that ^{18}F-FHNP has high affinity toward ER and, more particularly toward ERβ, because the tumor-to-plasma ratio decreased by 70% ($P < 0.001$).

There have been several attempts to develop an ERβ PET tracer (*9,24*). Perhaps the most relevant one was ^{18}F-FEDPN, with a relative binding affinity of 8% for ERβ and a relative selectivity ERβ/ERα of 20 (*9*). Although our PET tracer ^{18}F-FHNP has a lower relative binding affinity and selectivity than ^{18}F-FEDPN, we were still able to observe modest blocking effects in this study, most likely due to the higher levels of ER in our target compared with the uterus and ovaries used in previous studies. In addition, the low defluorination of our compound might have also influenced the selective uptake by increasing tracer delivery over time

Although this study was performed with a SKOV3 human ovarian carcinoma cell line, it does not give any guarantees that the PET tracer will also work in a clinical setting. Therefore, these data need to be confirmed in other studies, preferably in models with higher ERβ expression such as genetically engineered cell lines expressing only ERβ. If successful, clinical trials are warranted to assess the potential clinical usefulness of ^{18}F-FHNP.

CONCLUSION

^{18}F-FHNP can be readily radiolabeled with ^{18}F in high yield, providing a product with high specific activity. In vitro binding studies indicated that ^{18}F-FHNP has a higher affinity toward ERβ than ERα. PET imaging studies show that ERβ-expressing tumors can be clearly visualized with ^{18}F-FHNP PET. Moreover, in vivo studies with ^{18}F-FHNP confirm that the tracer has a preferential affinity toward ERβ. These promising preclinical results warrant further preclinical and clinical studies to confirm whether this PET tracer is indeed suitable for ERβ imaging.

DISCLOSURE

This study was funded by Mammoth project of the Center for Translational Molecular Medicine (CTMM). No other potential conflict of interest relevant to this article was reported.

ACKNOWLEDGMENTS

We gratefully thank Dr. Hetty Timmer-Bosscha for providing the cells and all the advice given during this study; Jurgen Sijbesma, Andrea Parente, and Alexandre Shoji for helping in the in vivo study; and Mohammed Khayum and Ate Boerema for assisting with the immunohistochemistry-western blotting assays. We also gratefully thank Dr. Fernanda Marques and Dr. Cristina Oliveira from Instituto Tecnológico e Nuclear, Portugal, for performing the in vitro binding assays with ERs.

REFERENCES

1. van Kruchten M, de Vries EG, Brown M, et al. PET imaging of oestrogen receptors in patients with breast cancer. *Lancet Oncol.* 2013;14:e465–e475.
2. Minutolo F, Macchia M, Katzenellenbogen BS, Katzenellenbogen JA. Estrogen receptor β ligands: recent advances and biomedical applications. *Med Res Rev.* 2011;31:364–442.
3. Fox EM, Davis RJ, Shupnik MA. ERβ in breast cancer: onlooker, passive player, or active protector? *Steroids.* 2008;73:1039–1051.
4. Pettersson K, Delaunay F, Gustafsson JA. Estrogen receptor bold beta acts as a dominant regulator of estrogen signalling. *Oncogene.* 2000;19:4970–4978.
5. Marcom PK, Isaacs C, Harris L, et al. The combination of letrozole and trastuzumab as first or second-line biological therapy produces durable responses in a subset of HER2 positive and ER positive advanced breast cancers. *Breast Cancer Res Treat.* 2007;102:43–49.
6. Smith IE, Walsh G, Skene A, et al. A phase II placebo-controlled trial of neoadjuvant anastrozole alone or with gefitinib in early breast cancer. *J Clin Oncol.* 2007;25:3816–3822.
7. van Kruchten M, de Vries EF, Arts HJG, et al. Molecular imaging of ER expression in epithelial ovarian cancer. *J Nucl Med.* 2015;56:50–55.
8. van Kruchten M, Glaudemans AW, de Vries EF, et al. PET imaging of estrogen receptors as a diagnostic tool for breast cancer patients presenting with a clinical dilemma. *J Nucl Med.* 2012;53:182–190.
9. Yoo J, Dence CS, Sharp TL, Katzenellenbogen JA, Welch MJ. Synthesis of an estrogen receptor β-selective radioligand: 5-[^{18}F]fluoro-(2R*,3S*)-2,3-bis(4-hydroxyphenyl)pentanenitrile and comparison of in vivo distribution with 16α-[^{18}F]fluoro-17β-estradiol. *J Med Chem.* 2005;48:6366–6378.
10. Niikawa H, Suzuki T, Miki Y, et al. Intratumoral estrogens and estrogen receptors in human non-small cell lung carcinoma. *Clin Cancer Res.* 2008;14:4417–4426.
11. Taniuchi S, Fujishima F, Miki Y, et al. Tissue concentrations of estrogens and aromatase immunolocalization in interstitial pneumonia of human lung. *Mol Cell Endocrinol.* 2014;392:136–143.
12. Mewshaw RE, Edsall RJ Jr, Yang C, et al. ERβ ligands. 3. Exploiting two binding orientations of the 2-phenylnaphthalene scaffold to achieve ERβ selectivity. *J Med Chem.* 2005;48:3953–3979.
13. Cole EL, Stewart MN, Littich R, Hoareau R, Scott PJH. Radiosyntheses using fluorine-18: the art and science of late stage fluorination. *Curr Top Med Chem.* 2014;14:875–900.
14. Mossine AV, Brooks AF, Makaravage KJ, et al. Synthesis of [^{18}F]arenes via the copper-mediated [^{18}F]fluorination of boronic acids. *Org Lett.* 2015;17:5780–5783.
15. Malik N, Solbach C, Voelter W, Machulla HJ. Nucleophilic aromatic substitution by [^{18}F]fluoride at substituted 2-nitropyridines. *J Radioanal Nucl Chem.* 2010;283:757–764.
16. Römer J, Füchtner F, Steinbach J, Johannsen B. Automated production of 16α-[^{18}F]fluoroestradiol for breast cancer imaging. *Nucl Med Biol.* 1999;26:473–479.
17. Antunes IF, Haisma HJ, Elsinga PH, Dierckx RA, de Vries EF. Synthesis and evaluation of [^{18}F]-FEAnGA as a PET tracer for beta-glucuronidase activity. *Bioconjug Chem.* 2010;21:911–920.
18. Neto C, Oliveira MC, Gano L, et al. Novel 7alpha-alkoxy-17alpha-(4′-halophenylethynyl)estradiols as potential SPECT/PET imaging agents for estrogen receptor expressing tumours: synthesis and binding affinity evaluation. *Steroids.* 2012;77:1123–1132.
19. Antunes IF, Haisma HJ, Elsinga PH, et al. Induction of β-glucuronidase release by cytostatic agents in small tumors. *Mol Pharm.* 2012;9:3277–3285.
20. Boerema AS. The brain at low temperature: neuronal & behavioural dynamics in mammalian hibernation and torpor. University of Groningen website. http://hdl.handle.net/11370/b6160376-d3b8-4e3e-baa6-775c2598863e. 2012. Accessed March 1, 2017.
21. Long X, Nephew KP. Fulvestrant (ICI 182,780): dependent interacting proteins mediate immobilization and degradation of estrogen receptor. *J Biol Chem.* 2006;.281:9607–9615.
22. Kuiper GG, Carlsson B, Grandien K, et al. Comparison of the ligand binding specificity and transcript tissue distribution of estrogen receptors alpha and beta. *Endocrinology.* 1997;138:863–870.
23. O'Donnell AJM, Macleod KG, Burns DJ, Smyth JF, Langdon SP. Estrogen receptor-α mediates gene expression changes and growth response in ovarian cancer cells exposed to estrogen. *Endocr Relat Cancer.* 2005;12:851–866.
24. Lee JH, Peters O, Lehmann L, et al. Synthesis and biological evaluation of two agents for Imaging estrogen receptor β by positron emission tomography: challenges in PET imaging of a low abundance target. *Nucl Med Biol.* 2012;39:1105–1116.